Fragile granular jamming

M. M. Bandi,[1] M. K. Rivera,[2] F. Krzakala,[3,4] and R. E. Ecke[4,*]

[1]*T-CNLS & MPA-10, Los Alamos National Laboratory, Los Alamos, NM 87545, USA*
[2]*D-4, Los Alamos National Laboratory, Los Alamos, NM 87545, USA*
[3] *CNRS and ESPCI ParisTech, 10 rue Vauquelin, UMR 7083 Gulliver, Paris 75000 France*
[4]*T-CNLS, Los Alamos National Laboratory, Los Alamos, NM 87545, USA*
(Dated: October 13, 2009)

We demonstrate experimentally that the route to a jammed state for a set of bi-dispersed frictional disks, subjected to uni-axial compression from a random initial unjammed state, consists of a consolidation state, a fragile jammed state, and finally a rigid jammed state. In the consolidation regime, the pressure on the sides increases very slowly with the packing fraction ϕ and there are no detectable stress chains. In the fragile jammed state, stress chains are visible, the pressure increases exponentially with ϕ, and the fraction of moving disks drops exponentially. Eventually, a final regime where particle displacements are below our resolution and the pressure varies approximately linearly with ϕ is reached. We argue that this scenario is generic for athermal frictional compressed particles.

PACS numbers: 64.60.-i,83.80.Fg,45.70.-n

When loose granular matter is progressively compressed to higher packing fractions ϕ, the material stiffens at a critical packing fraction ϕ_c owing to development of inter-particle constraints - the system is then said to be jammed. This transition from an athermal, particulate gas to a disordered solid has been related to the behavior of a wide variety of materials including glasses, foams, and colloids in a unifying phase diagram proposed by Liu and Nagel [1, 2]. From the perspective of real granular materials, however, the effects of inter-particle friction on the jamming scenario have not been widely considered [3]. On the contrary, to allow better comparison with the frictionless model, various empirical protocols such as mechanical shaking, repeated cycling, or high-pressure compaction (useful for relatively soft deformable particles) have been introduced in experimental systems to help break down weak frictional contacts. Nevertheless, friction can play a significant role in such materials, many of which are technologically relevant (as in the compression and sintering of ceramic [4]). It is thus important to understand the full impact of frictional contacts without resorting to mechanical vibration or repeated cycling whose effects are difficult to quantify.

Experiments [5, 6] have confirmed many features of the jamming transition, such as power-law scaling of the pressure P and of the mean coordination number Z with increasing ϕ [5], and a maximum in the pair-correlation function [6]. Given the unquantified mechanical vibration, cycling or highly-plastic deformation employed in the experimental work, an analysis of results that are strictly athermal, are weakly deformed during compression, and that fully manifest frictional effects is called for.

In this Letter, we report a quasi-static experiment across the jamming threshold, performed on a two-dimensional bidisperse system of photo-elastic disks. We show that the pressure scaling is remarkably different between the first and subsequent jamming cycles. In the first cycle as the system's boundaries are moved in to achieve an increasingly tighter packing, the pressure exhibits a short ramp followed by an exponential rise $P \propto e^{\phi/\chi_P}$. Eventually the pressure deviates from exponential behavior and scales linearly with respect to the packing fraction $P \propto \phi$. When decompressed and compressed again, however, the intermediate region with exponential scaling disappears and one recovers the approximate linear scaling [10]. The exponential increase in the pressure is reflected in an exponential decrease of the mean and variance of the domain size enclosed by stress chains above a certain cutoff and in an exponential decrease of the variance of particle displacements and of the fraction of particles moving more than about 1% of a particle diameter. Our measurements demonstrate that there are three regimes of frictional jamming during the first lateral compression: a consolidation regime where particles move freely; a *fragile* jammed region where pressure increases exponentially, particle displacements become smaller and less frequent, and a stress chain network forms; and finally a fully jammed state with approximately linear dependence of pressure on area fraction, very small displacements of bulk clusters, and an approximately static stress chain network. Measurements were also performed on disks machined with varying friction coefficients (Lexan, Teflon, and photo-elastic disks coated with graphite dust). The intermediate regime with an exponential rise in P was observed in all measurements over the same range of pressure, with exponents χ_P varying with the material bulk modulus. These results will be discussed in detail elsewhere.

Experimental set-up — Figure 1 shows a schematic of the experimental setup. The system consists of a bi-disperse mixture of 950 large (diameter $D = 0.9525 \pm 0.0025$ cm) and 950 small (diameter $d = 0.635 \pm 0.0025$ cm) polymer disks of thickness 0.508 cm that are bi-refringent under stress (photo-elastic). The disks are placed in a chamber, with dimensions $L = 25.9$ cm and $W = 48.2$ cm where L is the compression direction, consisting of two glass plates held 0.635 cm apart by means of an acrylic frame that runs along the system's perimeter. Two movable boundaries are placed on the acrylic frame with aluminum plates that can slide back-

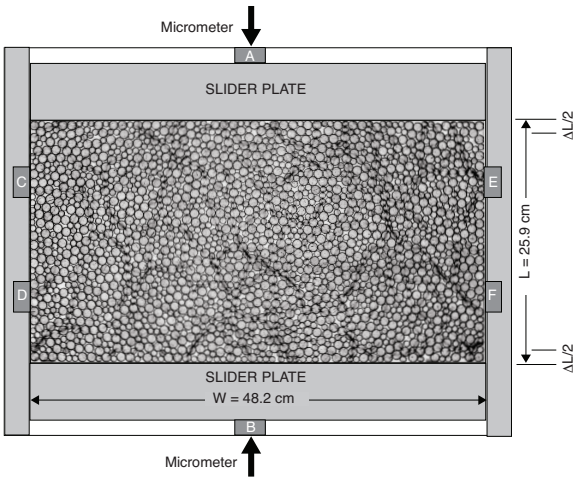

FIG. 1: Schematic of the experimental setup. The system consists of 950 large and 950 small disks (ratio of radii 1:1.5). Two movable boundaries at opposite ends control the system's packing fraction. Force sensors labeled A through F in the schematic measure the boundary pressure. The image is contrast enhanced data for $\phi = 0.8113$.

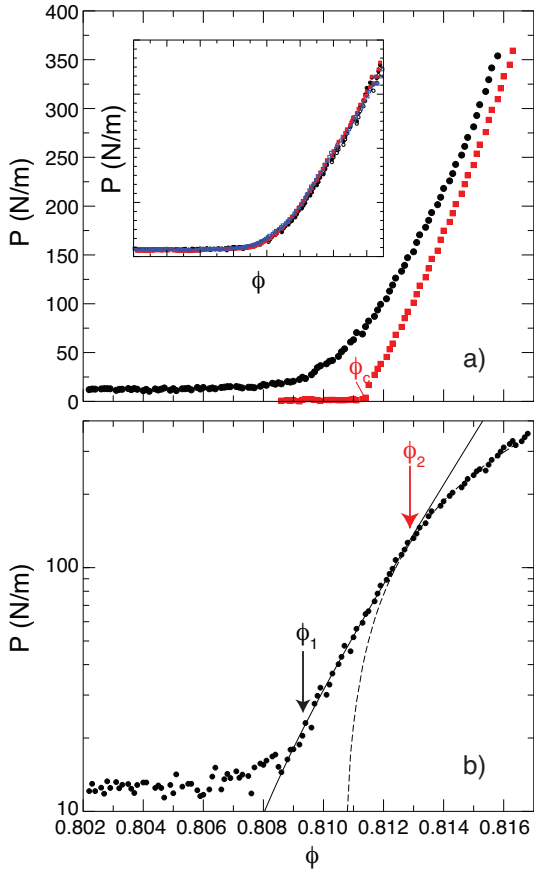

FIG. 2: (Color online) (a) P vs ϕ - linear scale - for the first (solid circles) and second (solid squares) jamming cycles. The pressure scaling is gradual for the first cycle as compared to the more abrupt transition during the second cycle where ϕ_c is indicated. The inset plots the pressure from all four boundaries (same vertical and horizontal scale). No anisotropy is observed in the pressure signal. (b) P vs ϕ for the first jamming cycle - log-linear scale - shows the existence of an intermediate regime where pressure scales exponentially. The solid line is an exponential fit to the data $P \propto e^{\phi/\chi_P}$ with $\chi_P = 0.002$, and the dashed line is a linear fit. Values of ϕ_1 and ϕ_2 are indicated in the plot.

and-forth within the chamber from opposite ends. The transverse boundaries are held fixed. The positions of the movable boundaries is controlled by two micrometers with a precision of 0.001 cm. Taking variations in radii into account for the given system of 1900 disks, this translates to a precision $\Delta\phi = 1 \times 10^{-5}$ in the packing fraction, and hence serves as the lower bound on the quasi-static step-size ($\Delta\phi$). All measurements reported in this letter, however, were made at a quasi-static step-size of $\Delta\phi = 1 \times 10^{-4}$. The packing fraction ($\phi$) is defined as the ratio of the area occupied by the disks to the total chamber area. The packing fraction is therefore controlled by changing the chamber area in this experiment. A set of six sensors (labeled A through F in Fig. 1) placed along the boundaries measure the global pressure. The noise floor of these sensors is of the order of 0.1 N/m. Along the compression direction, the sensors feel the friction of the movable boundaries with the glass bottom, which was measured to be about 11 N/m, accordingly this serves as the true zero of pressure measured along the compression axis. Visual measurements using a Nikon D-90 camera (12.3 megapixel resolution) yield positions and displacements of individual disks as well as the stresses inferred from the photo-elastic response of the disks [5]. We determined the local disk contacts having a stress above our experimental light intensity threshold (corresponding to about 1 N) and satisfying local force balance constraints. The entire stress chain network satisfies physical constraints and provides a good characterization of the distribution of local forces to complement the pressure measurements.

Protocol — We initially place all disks in the interrogation chamber in random positions and move the boundary plates to an initial packing fraction chosen *a priori* to fall comfortably in an unjammed state. The disks are subject to friction (both with the bottom boundary and with each other) and the system jams below the random close packed density $\phi_{rcp} = 0.838$. After each quasi-static step, a 10 s time-trace of all six boundary sensors is collected at a sampling frequency of 1 KHz followed by a digital image of the whole system. The time-averaged value of the trace constitutes the pressure measured by the boundary sensor at a particular value of ϕ. The boundaries are then moved through a quasi-static step ($\Delta\phi = 1 \times 10^{-4}$), and the procedure is repeated. We do not tap/anneal the system after each quasi-static step —as is often done in numerics— nor do we excite the system vibrationally to breakdown frictional effects: we are interested in studying the system evolution at "zero temperature" as it occurs under the control of a single parameter, namely ϕ.

Three regimes — The argument for a new, intermediate, fragile state is best appreciated by comparing the pressure signal for the first and second jamming cycles. Figure 2(a) plots

P from one compression boundary sensor versus ϕ for the first and second jamming cycles. The continuous increase in P for the first cycle is qualitatively different from the more abrupt change in slope for the second cycle. The lateral shift in P is a signature of a friction-induced hysteretic response which progressively shifts ϕ_c to higher values as the system is repeatedly jammed and unjammed (discussed in detail elsewhere). The vertical shift in P in the unjammed regime for the first cycle is traced to the friction between the movable boundary plates and the glass bottom. During the first cycle, the boundaries move in and push the disks towards a jammed configuration. When unjammed and jammed again, the contacts that were developed at the end of the first jamming cycle are re-activated, and the stresses build up as the system is subjected again to uni-axial compression.

In order to better understand the smooth increase in P for the first jamming cycle, Fig. 2(b) plots P versus ϕ on a log-linear scale. One sees three distinct regimes in the pressure curve. In the unjammed (consolidation regime) P is essentially flat, modulo a shallow ramp due to friction between disks and bottom glass plates. The second regime is characterized by an exponential increase in P beginning at $\phi_1 \approx 0.8093$. The solid line in Fig. 2(b) is an exponential fit to the data $P \propto e^{\phi/\chi_P}$ with $\chi_P = 0.002$. The pressure eventually deviates from this exponential regime and settles to a linear scaling $P \propto \phi$ at $\phi_2 = 0.8124$. The inset in Fig. 2 (a) plots P from all four boundaries against ϕ on a log-linear scale. The remarkably good collapse of the pressure curves atop one another strongly suggests that anisotropic effects arising from uni-axial compression are not detected by the pressure sensors. This isotropy may result from our geometry for which the aspect ratio is $L/W = 0.54$ and would probably not persist for large aspect ratios, i.e., $L/W >> 1$.

This exponential pressure scaling for the first jamming cycle contradicts the predicted [5, 7, 8] power-law for P across the jamming transition. This power-law scaling (approximately linear [10]) is, however, recovered for subsequent jamming cycles as shown for the second jamming cycle in Fig. 2a where $\phi_c = 0.8113$ is determined by the point at which P starts to rise.

To elucidate the nature of the different regimes that we observe in global pressure measurements, we consider local properties of disk configurations, namely the structure of stress chains and the measurements of disk displacements. The identified stress chains enclose domains with no measured stress as illustrated in the insets of Fig. 3. We characterize the stress chain networks by the mean a_m and variance a_v of the fractional domain area (relative to the total cell area on the left axis) and also by the mean $\tilde{a}_m$ and variance $\tilde{a}_v$ of the domain area but now normalized (right axis) by the average of the area enclosed by a triangular arrangement of small and large disks (all large, all small, two large, two small). As indicated in the inset images, the mean and variance decrease rapidly between 0.810 (the lowest value of ϕ for which we could determine the stress chain network) and $\phi_2 = 0.8124$. For higher $\phi > 0.8124$, the mean and variance decrease linearly with a small slope. Fits to an exponentially decreasing function $e^{-\phi/\chi_s}$ as shown in Fig. 3 yields the same value of $\chi_s = 0.00035$. The exponential decrease in a_m and a_v is another signature of the fragile jammed state.

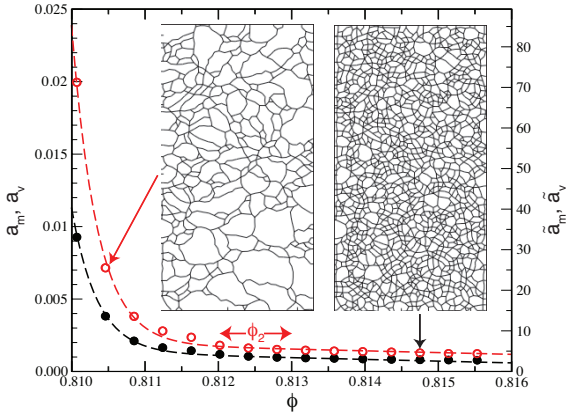

FIG. 3: (Color Online) Mean (•)and variance (○) of stress chain domain area normalized by total area, a_m, a_v (left axis) or by the mean area formed by connections between different combinations of 3 disks in a close packed triangular array, $\tilde{a}_m$, $\tilde{a}_v$ (right axis), respectively. Insets show stress networks and corresponding domains for $\phi = 0.8104$ (left) and $\phi = 0.8148$ (right). The dashed lines are fits to a combined linear dependence with a decaying exponential (see main text).

We now consider the behavior of disks displacements. Figure 4a shows the fraction of disks moving a distance greater than about 1% of a mean disk diameter [12] as a function of ϕ where N_m is the number moving and $N_T = 1900$ is the total number of disks. The fraction is constant at about 0.3 up to $\phi_1 = 0.8094$, after which it decreases rapidly up to the jamming value $\phi_2 = 0.8123$. The decrease is consistent with an exponential $e^{-\phi/\chi_N}$ with $\chi_N \approx 0.001$. The variance of individual disk displacements σ (normalized by $\tilde{d} = (D + d)/2 = 0.794$ cm) relative to a state near the jamming threshold [11] is shown in Fig. 4 as a function of ϕ. One again observes two distinct regimes: a linear one that corresponds to the unjammed (consolidation) regime where the pressure curve in Figure 2(b) is flat, and a second one in which the variance decreases exponentially with $\sigma \propto e^{-\phi/\chi_\sigma}$ with $\chi_\sigma = 0.0007$. This exponential drop in displacement variance occurs over the same interval in ϕ as the exponential regime of the pressure curve in Fig. 2(b) as indicated by the arrows depicting ϕ_1 and ϕ_2. The presence of disk displacements in the exponential regime, where a percolating force network already exists, suggests that the particles that are part of the force network still undergo small displacements and deformations, which in turn allows visible displacement *inside* the network region, eventually leading to the refining of the network. This picture is reinforced by the data in the inset of Fig. 4(b) where the difference in the force chain network between $\phi = 0.8095$ and $\phi = 0.8105$ is shown as black lines and the spatial distribution of the magnitude of particle displacements is also shown: The correlation of new stress chain creation

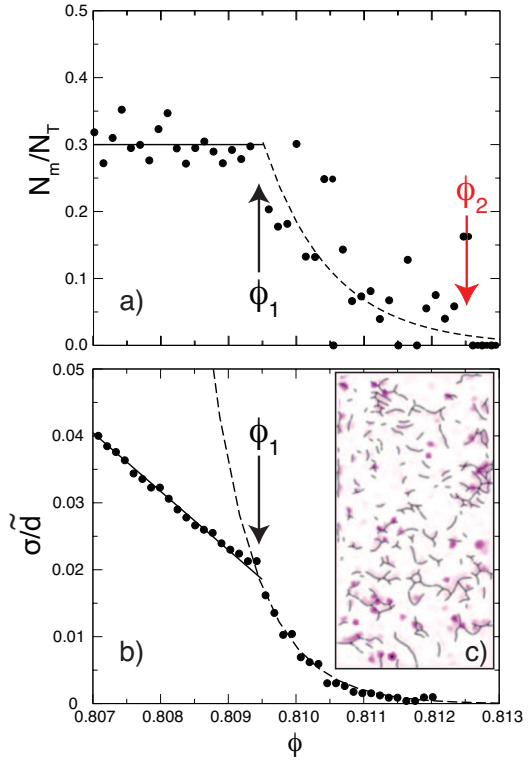

FIG. 4: (Color online) (a) Fraction of disks moving N_m/N_T vs ϕ showing constant region for $\phi < \phi_1$ and exponential decay for $\phi_1 < \phi < \phi_2$ with $\chi_N \approx 0.001$. (b) Normalized displacement variance $\sigma/\tilde{d}$ relative to a state near ϕ_2 showing a linear decrease for $\phi < \phi_1$ and an exponential decrease with $\chi_\sigma = 0.0007$ for $\phi_1 < \phi < \phi_2$. (c) Image of the superposition of the difference in the stress network (black lines) and the magnitude of disk displacements between $\phi = 0.8095$ and $\phi = 0.8105$ Arrows indicate ϕ_1 and ϕ_2.

(the differences) and the particle displacements is striking.

Figures 2 and 4, when considered together, present a picture of a fragile system where part of the system is jammed (as evidenced by an exponential increase in pressure) whereas another part is still floppy (as seen from the variance of disk displacements, albeit decreasing exponentially with ϕ, and the corresponding decrease in the mean and variance of domain area in Fig. 3). These results collectively form the crux of the argument presented in this Letter arguing in favor of a fragile jammed state that separates the unjammed and the rigid one.

Discussions — We have presented compelling evidence for the existence of an intermediate fragile state separating the unjammed consolidation state from the rigid jammed state of athermal particles with frictional contacts. The fragile state is characterized by an exponential rise in pressure against a power-law scaling predicted by field theories [8], simulations [7] and experiments that minimize friction through external perturbations or cycling [5]. Friction seems to play an essential role in providing the mechanical support leading to a marginally stable, yet fragile solid. These findings may be related to the experiments of Ref.[6] where the pressure shows a similar smooth rise in a very different system, suggesting that our scenario is a generic one for athermal frictional compressed particles.

Comparing the exponential behaviors of different quantities in the fragile jammed state provides an interesting but incomplete part of our work. Since $\chi_s = 0.00035$ measures the behavior of domain area, a domain length $\ell = \sqrt{a_m}$ would be expected to have twice the decay constant (owing to the square root) or 0.0007. This is just the value of χ_σ. One might argue that the global pressure is some average over the network stress chain, say $P \sim \sum F_{sc}/\ell$, which implies that forces would increase exponentially with $\chi_F \sim 0.002 - 0.0007 = 0.0013$. It would also be interesting to see if there is any relation between the intermediate regime and the so-called intermediate phase that occurs in rigidity percolation [9]. In both cases, a direct and precise measurement of stress chain magnitudes would allow a quantitative test. In any event, the robust exponential behavior observed here experimentally certainly calls out for a theoretical explanation.

This work was carried out under the auspices of the National Nuclear Security Administration of the U.S. Department of Energy at Los Alamos National Laboratory under Contract No. DE-AC52-06NA25396.

* Corresponding Author: ecke@lanl.gov

[1] A. Liu and S. Nagel, Nature **396**, 21 (1998).
[2] C. Song, P. Wang , H.A. Makse, Nature **453**, 629 (2008).
[3] F. Radjai *et al*, Phys. Rev. Lett. **77**, 274 (1996). L. Silbert *et al*, Phys. Rev. E **65**, 031304 (2002). E. Somfai *et al*, Phys. Rev. E **75**, 020301(R) (2007). K. Shundyak *et al*, Phys. Rev. E **75**, 010301(R) (2007).
[4] D. Cumberland and R. Crawford, *The packing of particles*, Elsevier Science, New York, USA (1987).
[5] T. Majmudar *et al.*, Phys. Rev. Lett. **98**, 058001 (2007).
[6] X. Cheng, arXiv:0905:2788v1 (2009).
[7] C. O'Hern *et al.*, Phys. Rev. E. **68**, 011306 (2003).
[8] S. Henkes and and B. Chakraborty, Phys. Rev. Lett. **95**, 198002 (2005).
[9] M. F. Thorpe *et al.*, J. Non-Cryst. Solids **266**, 859 (2000).
[10] The best fit of the data to the form $P \propto (\phi - \phi_c)^\beta$ yields $\beta = 1.1$, consistent with [5].
[11] Picking different reference states near or beyond jamming causes a finite offset in variance of different magnitudes, but the exponential decay is preserved with the same value of $\chi = 0.0007$ to within experimental precision.
[12] There are smaller displacements below our threshold that may behave differently as a function of ϕ.